European Journal of Medicinal Chemistry 46 (2011) 370–377

Contents lists available at ScienceDirect

European Journal of Medicinal Chemistry

journal homepage: http://www.elsevier.com/locate/ejmech

Short communication

Penetratin analogues acting as antifungal agents

Francisco M. Garibotto [a,b], Adriana D. Garro [a,b], Ana M. Rodríguez [a], Marcela Raimondi [c,d], Susana A. Zacchino [c], Andras Perczel [e], Csaba Somlai [f], Botond Penke [f], Ricardo D. Enriz [a,b,*]

[a] Facultad de Química, Bioquímica y Farmacia, Universidad Nacional de San Luis, Chacabuco 915, 5700 San Luis, Argentina
[b] IMIBIO-SL, CONICET. Chacabuco 915, 5700 San Luis, Argentina
[c] Facultad de Ciencias Bioquímicas y Farmacéuticas, Farmacognosia, Universidad Nacional de Rosario, Suipacha 531, Rosario 2000, Argentina
[d] Facultad de Ciencias Médicas, Microbiología, Universidad Nacional de Rosario, Suipacha 531, Rosario 2000, Argentina
[e] HAS-ELU Protein Modelling Group, Institute of Chemistry, Eötvös L. University Pázmány P. s. 1/a Budapest, Hungary
[f] Department of Medical Chemistry, University of Szeged H-6720 Szeged, Dóm tér 8, Hungary

ARTICLE INFO

Article history:
Received 27 July 2010
Received in revised form
21 October 2010
Accepted 26 October 2010
Available online 29 October 2010

Keywords:
Antifungals
Candida albicans
Conformational study
Cryptococcus neoformans
Molecular electrostatic potentials
Peptides

ABSTRACT

The synthesis, *in vitro* evaluation, and conformational study of penetratin analogues acting as antifungal agents are reported. Different peptides structurally related with penetratin were evaluated. Analogues of penetratin rich in Arg, Lys and Trp amino acids were tested. In addition, HFRWRQIKIWFQNRRM[O]KWKK-NH_2, a synthetic 20 amino acid peptide was also evaluated. These penetratin analogues displayed antifungal activity against human pathogenic strains including *Candida albicans* and *Cryptococcus neoformans*. In contrast, Tat peptide, a well-known cell penetrating peptide, did not show a significant antifungal activity against fungus tested here. We also performed a conformational study by means experimental and theoretical approaches (CD spectroscopic measurements and MD simulations). The electronic structure analysis was carried out from Molecular Electrostatic Potentials (MEP) obtained by using RHF/6-31G *ab initio* calculations. Our experimental and theoretical results permitted us to identify a topographical template which may provide a guide for the design of new peptides with antifungal effects.

1. Introduction

Many fungal infections are caused by opportunistic pathogens that may be endogenous (*Candida* infections) or acquired from the environment (*Cryptococcus, Aspergillus* infections). Patients with significant immunosuppression frequently develop *Candida* esophaguitis. Cryptococcosis, caused by the encapsulated yeast *Cryptococcus neoformans* (*C. neoformans*), has been the cause of fungal mortality among HIV-infected patients [1]. This organism has predilection for the central nervous system and leads to severe, life-threatening meningitis. Although it appears that many drugs are available for the treatment of systemic and superficial mycoses, there are in fact only a limited number of efficacious antifungal drugs [2]. Azoles that inhibit sterol formation and polyenes that bind to mature membrane sterols have been the mainstays of antifungal therapy for the last two decades [3]. However, the emergence of azole resistance among different pathogenic strains and the high toxicity of amphotericin B [4,5] have prompted research for new antifungal agents [6]. Although combination therapy has emerged as a good alternative to bypass these disadvantages [7,8], there is a real need for a next generation of safer and more potent antifungal agents [2,8]. This event resulted in the identification of novel molecules, which might result useful for a future development.

Small cationic peptides [9,10] are abundant in nature and have been described as 'nature's antibiotics' or 'cationic antimicrobial peptides'. These peptides are 12–50 amino acids long with a net positive charge of +2 or +9, due to an excess of basic arginine and lysine, and with approximately 50% of hydrophobic amino acid residues [9]. Penetratin, a well-known cell penetrating peptide (CPP) and a synthetic 16 amino acid peptide from the third helix of *Antennapedia homeodomain* [11], is a cationic amphipathic peptide which might penetrate cell membranes *via* a postulated 'inverted micelle' pathway [12]. This peptide has been proposed as a universal intracellular delivery vehicle. Recently, we have reported that penetratin showed antifungal activity against *Candida albicans (C. albicans)* and *C. neoformans* [13].

In the present report, we extend our previous studies analyzing different peptides structurally related to penetratin. Two principal

* Corresponding author. Facultad de Química, Bioquímica y Farmacia, Universidad Nacional de San Luis, Chacabuco 915, 5700 San Luis, Argentina. Tel.: +54 2652 423789; fax: +54 2652 431301.
E-mail address: denriz@unsl.edu.ar (R.D. Enriz).

0223-5234/$ – see front matter © 2010 Elsevier Masson SAS. All rights reserved.
doi:10.1016/j.ejmech.2010.10.025

goals were initially proposed for this work: i) to synthesize and test new analogues of penetratin, and ii) to measure the antifungal capacity of Tat peptide (another well-known CPP).

We also performed a conformational analysis from both experimental (circular dichroism, CD) and theoretical methods (Electrostatically Driven Monte Carlo (EDMC) calculations and Molecular Dynamics (MD) simulations). Conformational and electronic analyses were performed in order to confirm the pharmacophoric pattern recently reported for these antifungal peptides [13,14].

2. Experimental

2.1. Synthetic methods

Solid phase synthesis of the peptides was carried out manually on a *p*-methyl benzhydrylamine resin (1 g MBHA, 0.14 mmol/g) with standard methodology using Boc-strategy. Side chain protecting groups were as follows: Arg(Tos), Lys(2Cl-Z), Cys(Mbzl), Tyr (2-Br-Z). All protected amino acids were coupled in CH_2Cl_2 (5 ml) using DCC (2.5 equiv.) and HOBt (2.5 equiv.) until completion (3 h) judged by Kaiser [15] ninhydrin test. After coupling of the appropriate amino acid, Boc deprotection was effected by use of TFA/CH_2Cl_2 (1:1, 5 ml)) for 5 min first then repeated for 25 min. Following neutralization with 10% TEA/CH_2Cl_2 three times (5-5 ml of each), the synthetic cycle was repeated to assemble the resin-bond protected peptide. The peptides were cleaved from the resin with simultaneous side chain deprotection by acidolysis with anhydrous hydrogen fluoride (5 ml) containing 2% anisole, 8% dimethyl sulfide and indole at 5 °C for 45 min. The crude peptides were dissolved in aqueous acetic acid and lyophilized. Preparative and analytical HPLC of the crude and the purified peptides were performed on an LKB Bromma apparatus (for preparative HPLC, column: Lichrosorb RP C18, 7 μm, 250 × 16 mm; gradient elution: 30–100%, 70 min; mobile phase: 80% acetonitrile, 0.1% TFA; flow rate: 4 ml/min, 220 nm, for analytical HPLC, column: Phenomenex Luna 5C18(2), 250 × 4.6 mm; mobile phase: 80% acetonitrile, 0.1% TFA; flow rate: 1.2 ml/min, 220 nm, ESI-MS: Finnigan TSQ 7000.

HPLC data of the synthesized peptides

	Retention factor (min)	Gradient elution (%)
RQIRIWFQNRRMRWRR-NH_2 (**2**)	8.808	25–40 (15 min)
KQIKIWFQNKKMKWKK-NH_2 (**3**)	11.510	20–40 (20 min)
RWWKWWWWWRRWKWKK-NH_2 (**4**)	6.026	35–50 (15 min)
YGRKKRRQRRRC-NH_2 (**5**)	6.898	12–27 (15 min)
HFRWRQIKIWFQNRRM[O]KWKK-NH_2 (**6**)	5.775	28–43 (15 min)

The instrument for ESI-MS was Finnigan TSQ 7000 and the data are as follows: (**2**) 590 (M/4+1), 518 (M/5+2Na^+), 495 (M/5 + Na^+), 472 (M/5 + 1), 394 (M/6 + 1); (**3**) 1081 (M/2 + 1), 721 (M/3 + 1), 541 (M/4 + 1), 433 (M/5 + 1); (**4**) 892 (M/3 + 1), 670 (M/4 + 1), 536 (M/5 + 1); (**5**) 832 (M/2 + 1), 555 (M/3 + 1), 416 (M/4 + 1), 356 (M/5 + Na^+), 333 (M/5 + 1); (**6**) 964.0 (M/3 + 1), 723.2 (M/4 + 1), 578.8 (M/5 + 1), 482.1 (M/6 + 1).

2.2. Microorganisms and media

Strains of *C. albicans* and *C.neoformans* from the American Type Culture Collection (ATCC, Rockville, MD, USA) were used. *C. albicans* ATCC 1 0231, and *C. neoformans* ATCC 32264 were grown on Sabouraud–chloramphenicol agar slants for 24 h at 35 °C, maintained on slopes of Sabouraud–dextrose agar (SDA, Oxoid). Inocula of cell suspensions were obtained according to reported procedures and adjusted to 1–5 × 10^3 cells with colony forming units (CFU)/mL [16].

2.3. Antifungal evaluation

The test was performed in 96 wells-microplates. Peptide test wells (PTW) were prepared with stock solutions of each peptide in DMSO (≤2%), diluted with RPMI-1640 to final concentrations 200–3.125 μM. Inoculum suspension (100 μl) was added to each well (final volume in the well = 200 μL). A growth control well (GCW) (containing medium, inoculum, the same amount of DMSO used in PTW, but compound-free) and a sterility control well (SCW) (sample, medium and sterile water instead of inoculum) were included for each strain tested. Microtiter trays were incubated in a moist, dark chamber at 35 °C, 24 or 48 h for *Candida* spp or *Cryptococcus* sp. respectively. Microplates were read in a VERSA Max microplate reader (Molecular Devices, Sunnyvale, CA, USA). Amphotericin B (Sigma Chemical Co, St Louis, MO, USA) was used as positive control (100% inhibition). Tests were performed by duplicate. Reduction of growth for each peptide concentration was calculated as follows: % of inhibition: 100- (OD_{405} PTW- OD_{405} SCW)/OD_{405} GCW - OD_{405} SCW.

2.4. Statistical analysis

Data were statistical analyzed by both, one-way analysis of variance and Student's test. A $p < 0.05$ was considered significant.

2.5. Computational methods

2.5.1. EDMC calculations

The conformational space was explored using the method previously employed by Liwo et al. [17] that included the EDMC method [18] implemented in the ECEPPAK [19] package. Conformational energy was evaluated using the ECEPP/3 force field [20]. Hydration energy was evaluated using a hydration-shell model with a solvent sphere radius of 1.4 Å and atomic hydration parameters that have been optimized using nonpeptide data (SRFOPT) [21]. In order to explore the conformational space extensively, 10 different runs were carried out, each of them with a different random number. Therefore, a total of 5000 accepted conformations were collected. Each EDMC run was terminated after 500 energy-minimized conformations had been accepted. The parameters controlling the runs were the following: a temperature of 298.15 K for the simulations; a temperature jump of 50 000 K, and the maximum number of allowed repetitions of the same minimum was 50. The maximum number of electrostatically predicted conformations per iteration was 400; the maximum number of random-generated conformations per iteration was 100; the fraction of random/electrostically predicted conformations was 0.30. The maximum number of steps at one increased temperature was 20; and the maximum number of rejected conformations until a temperature jump was executed was 100. Only *trans* peptide bonds ($\omega \cong 180°$) were considered. All accepted conformations were then clustered into families using the program ANALYZE [19] by applying the minimal-tree clustering algorithm for separation, using backbone atoms, energy threshold of 30 kcal mol^{-1}, and RMSD of 0.75 Å as separation criteria. This clustering step allows a substantial reduction of the number of conformations and the elimination of repetitions. A more detailed description of the procedure used here is given in section 4.4 Computational Methods of reference [13].

2.5.2. Molecular dynamics simulations

MD simulations were performed using a combined decane/water system which was previously used with success for other compounds of biological interest [22]. MD simulations and the trajectory analysis were performed using the GROMACS 3.3 programs package [23]. The GROMACS [24,25] united-atoms force field (FF) and the SPC water

model were used. The time step for the simulations was 0.002 ps. For long-ranged interactions, the particle-mesh Ewald (PME) [26] method was used with a 1 nm cutoff and a Fourier spacing of 0.12 nm. The MD protocol consisted of several preparatory steps: energy minimization using the conjugate gradient model [27], density stabilization (NVT conditions), and finally production of the MD simulation trajectory. All production simulations were performed under NPT conditions at 300.0 K and 1.0 bar, using Berendsen's coupling algorithm [28] for keeping temperature ($\tau T = 0.1$ ps) and pressure ($\tau P = 0.5$ ps) constant. The compressibility was 4.8×10^{-5} bar^{-1}. All coordinates were saved every 5.0 ps. The SETTLE [29] algorithm was used to keep water molecules rigid during MD simulations. The LINCS [30] algorithm was used to constrain all length bonds in the preparatory steps. However, no restrains were used in production-MD simulations. A length of 50.0 ns was taken in to account for all production-MD simulations. The molecular system consisted of a biphasic environment in which the conformational behaviour of peptides were examined. This biphasic system consisted of 188 decane molecules and 1468 water molecules; the size of the simulation box was 4.36 nm in the *x* and *y* directions, and 5.42 nm in the *z* direction. This system was built up in such a way that all decane molecules were forming a layer located near the middle of the box (ca. 2.71 nm in the *z* direction) whereas water molecules were above and below the decane layer. The thickness of the decane layer was ~2.96 nm. Just then, the solvent (decane and water) molecules were correctly localized into the box. An energy minimization and an NVT-MD simulation of 10 ns long were performed in order to equilibrate the interfaces formed between solvent molecules. After the solvent stabilization was reached, a molecule of each peptide was embedded into the decane/water interface. An extra step of prestabilization of 1 ns long was performed before the production-MD simulation was started.

2.5.3. Molecular electrostatic potentials

Quantum mechanics calculations were carried out using the Gaussian 03 program [31]. We use the most populated conformations of peptides **2**–**5** obtained from EDMC calculations. Subsequently, single point *ab initio* (RHF/6-31G) calculations were carried out. The electronic study was carried out using molecular electrostatic potentials (MEP) [32]. These MEP were calculated using RHF/6-31G wave functions and MEP graphical presentations were created using the MOLEKEL program [33].

3. Results and discussion

On the basis of our results obtained for penetratin (RQIKIWFQNRRMKWKK-NH_2, peptide **1**) and its analogues acting as antifungal agents [13,14], as well as on previously reported structure–activity relationship studies performed on their penetrating capacity [34,35], we synthesized four different analogues of penetratin (compounds **2**–**4** and **6**). Tat peptide (YGRKKRRQRRR-NH_2, peptide **5**) was also included in this study. Previous reports have indicated that the presence of R and K amino acids are important for the antimicrobial effect of these peptides [9]. Therefore, we synthesized and tested peptides **2** and **3** which are analogues of **1** and are rich in R and K residues, respectively. Both compounds displayed antifungal activity against the tested fungus, particularly against *C. neoformans* showing a percentage of inhibition of 77% and 72% at a relatively low molar concentration (12.5 μM) (Table 1). In general, peptides **2** and **3** displayed a closely related antifungal activity with respect to that previously reported for **1**.

It has been demonstrated that the presence of a significant number of hydrophobic residues along the sequence of these cationic antimicrobial peptides is also of importance for their biological effect. Our recent results on small-size antifungal peptides

Table 1
Antifungal activity (% inhibition) of peptides **1**–**6** against *Candida albicans* ATCC 10231 and *Cryptococcus neoformans* ATCC 32264. The percentage of inhibition higher than 60, are denoted in bold.

Peptide	Candida albicans						Cryptococcus neoformans					
	200 μM	100 μM	50 μM	25 μM	12.5 μM	6.25 μM	200 μM	100 μM	50 μM	25 μM	12.5 μM	6.25 μM
1[a]	**100**	**100**	**95** ± 1.2	**91** ± 1.6	4.00 ± 0.1	0	**100**	**100**	**100**	**100**	**90** ± 2.3	**60** ± 2.40
2	**100**	**100**	**98.92** ± 1.28	6.16 ± 0.59	4.38 ± 1.97	3.71 ± 0.50	**100**	**100**	**100**	**81.74** ± 12.41	**77.53** ± 3.13	43.30 ± 2.06
3	**100**	**100**	**100**	8.41 ± 2.33	5.97 ± 0.71	3.24 ± 2.47	**100**	**100**	**100**	**98.52** ± 4.01	**72.03** ± 2.66	**64.45** ± 2.83
4	**100**	**99.11** ± 0.4	**95.84** ± 0.26	30.94 ± 0.73	14.75 ± 2.52	8.72 ± 2.32	**100**	**90.04** ± 0.33	**77.51** ± 4.37	44.18 ± 2.51	31.48 ± 2.70	22.56 ± 4.40
5	**99.08** ± 0.26	**99.10** ± 0.0	6.75 ± 2.50	6.71 ± 1.38	6.12 ± 0.76	4.97 ± 0.20	**100**	**100**	**61.30** ± 4.58	1.75 ± 0.48	0	0
6	**100**	**100**	**93.66** ± 0.84	5.96 ± 1.41	3.95 ± 1.00	2.90 ± 0.04	**100**	**100**	**100**	**100**	**99.35** ± 0.67	**95.06** ± 0.66
Amph. B[b]	100	100	100	100	100	100	100	100	100	100	100	100
Ket[c]	100	100	100	100	100	100	100	100	100	100	100	100

[a] previously reported in reference [13].
[b] Amphotericin B.
[c] Ketoconazole.

[14] are an additional support for such hypotheses. Thus, we decided to synthesize and test peptide **4**, which is an analogue of penetratin rich in Trp. However, peptide **4** displayed a lower antifungal activity against the tested fungi (Table 1) compared to penetratin.

Tat peptide (**5**), derived from the HIV Tat transactivator protein [36], was identified to efficiently cross the plasma membrane. On the basis of the above data, we decided to synthesize and evaluate peptide **5**. Our results indicated that this peptide possesses only a marginal antifungal activity against the fungi tested here, showing a percentage of inhibition of 100% at 100 μM against *C. neoformans* (Table 1). Thus, Tat displayed a markedly lower antifungal activity with respect to that obtained for penetratin.

We have previously reported that His-Phe-Arg-Trp-NH_2, the 6-9 sequential unit of α-MSH, and structurally related tetrapeptide showed antifungal properties especially against *C. neoformans* [37]. More recently we have reported that HFRWRQIKIWFQNRRMK WKK-NH_2 (the 6-13 sequence of α-MSH attached to penetratin) displayed significant antifungal activity against both *C. albicans* and *C. neoformans* [38]. In order to investigate if the replacement of methionine (M) residue by methionine sulfoxide (M[O]) might increase or decrease the antifungal effect, peptide **6** was synthesized and tested. Peptide **6** displayed the strongest antifungal effect against *C. neoformans* and a significant activity against *C. albicans* as well. Thus, it should be noted that peptide **6** was the most active peptide of this series.

In order to better understand the above experimental results, we performed an exhaustive conformational and electronic structure study of peptides **2**–**6**. In a first step the conformational analysis of these peptides was carried out using EDMC calculations [17]. These calculations were conducted in the same way as previously reported [13,14]. EDMC results predicted that peptides **2**–**5** possessed a tendency to adopt helix-like secondary structures, being an α-helix structure the most representative form for these peptides. These conformations were characterized by hydrogen bonds between the carbonylic oxygen (residue *i*) and the NH group (residue $i + 4$). The details of the EDMC results obtained for peptides **1**–**5** are given in Tables S1–S5 (Supplementary data). It is interesting to note that previous NMR studies suggested that the Tat peptide (**5**) is unstructured in solution [39] which is in disagreement with our EDMC results. In a previous work [13], we carried out an extensive conformational study of penetratin (**1**) using three different complementary approaches: molecular mechanics, simulated annealing and MD simulations. Comparing those results, we concluded that the three methods predicted a helix-like structure as the preferred form for peptide **1**. However, alternative studies have suggested that this peptide in solution is either partially α-helical [40,41] or has a partial β-hairpin structure [42]. On the other hand experimental CD studies have demonstrated that in a membrane-mimetic environment, penetratin [34] and analogues [38] displayed a clear tendency to form helix-like secondary structures. In the presence of such a situation a reasonable step to take is to look for theoretical calculations which simulate a membrane-mimetic environment. Thus, we performed MD simulations on a combined decane/water system which has been previously used to simulate a membrane-like phase [22].

Fig. 1 shows the change in the secondary structure during MD simulation for peptide **1**. In this simulation the residues 5 to 12 have shown the highest preference for α-helix conformation. In contrast, the initial and final residues appear to have a random coil structure because of the flexibility of these residues. Such a conformational behaviour was observed until the end of the simulation.

Fig. 2 shows a snapshot of the peptide **6**/decane/water system at the end of the MD simulation (25 ns) displaying the spatial orientation of this peptide in the membrane-like phase. Similar results

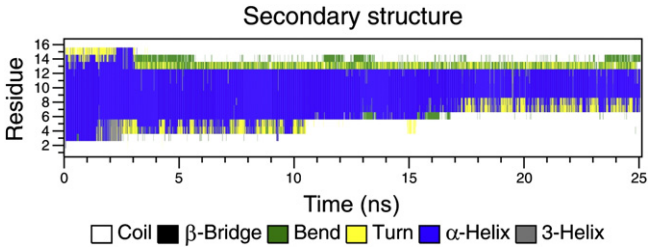

Fig. 1. Change in the secondary structure during molecular dynamics simulation for peptide 6.

were obtained for the rest of peptides reported here, being the results for peptide **1** representative of this series.

To corroborate these theoretical results, in the next step CD spectroscopic measurements were performed both in water and in a mixture of TFE and water (3:7) for peptide **6** which was the most active compound in this series. Peptide **6** was measured at room temperature by using the following conditions (pH adjusted by HCl/NaOH solutions); concentration: 0.023 mM; pH = 6.7.

The spectral analysis revealed that peptide **6** showed little or no structural preference in water (Fig. 3, black line). The "U"-type CD spectrum reflected the presence of a very large number of different local conformations in a time average manner. Therefore, in water, from the shape of this U-type CD curve little characteristic secondary structure content could be extracted for this peptide (black line). When peptide **6** was recorded in the solvent mixture of 30% TFE and 70% H_2O, a significant change in the shape of the curves was observed. The CD curve of peptide **6** (see red line in Fig. 3) had a spectral feature similar to those of a C-type CD curve. Thus, the "red curve" most probably reflected a conformational ensemble composed of α- or 3_{10}-helix combined with type I/III β-turns plus some percentage of still unstructured (or highly mobile) backbone foldamers. These results demonstrated that in the presence of a considerable amount of TFE, peptide **6** adopted an increased amount of helical and/or type I/III β-turn secondary structure. These results are in agreement with those previously reported for penetratin [34] and analogues [38].

To better characterize the spatial orientations of this peptide, we plotted Edmundson wheel representations of peptides **1**–**5** (Fig. 4). The wheel representations obtained for peptides **2** and **3** were very similar, showing two clearly differentiated façades: the 'charged one' (denoted in dash line in Fig. 4) and a more extended 'uncharged one' (denoted in full line). The first face identifies the cationic residues 11, 4, 15 and 1 (R or K) as those accounting for the mutual coulombic binding. The first three residues were located on the same side of the helical peptide, and we named that side 'charged face'. These positively charged residues at neutral pH were able to produce salt bridges with the anionic site of lipids. The uncharged face was more extensive and was formed by a total of six hydrophobic (M12, I5, W6, I3, W14 and F7) and two polar residues (N9 and Q2). The rest of the positively charged residues were homogeneously distributed. Thus, cationic residues 16, 13 and 10 were strategically intercalated along the 'uncharged façade'. In relation to the nomination used here for the two faces, two aspects deserve an explanation. The first one is that although the 'uncharged face' possesses some cationic residues, we decided to call it 'uncharged' in order to differentiate this moiety, possessing more hydrophobic and polar amino acid residues, from the so-called 'charged face'. The second point is that W is assumed to be a hydrophobic amino acid. This is not totally correct as W can form hydrogen bonds and induce dipole interactions. However, for our purposes such assumption might be considered a reasonable approach.

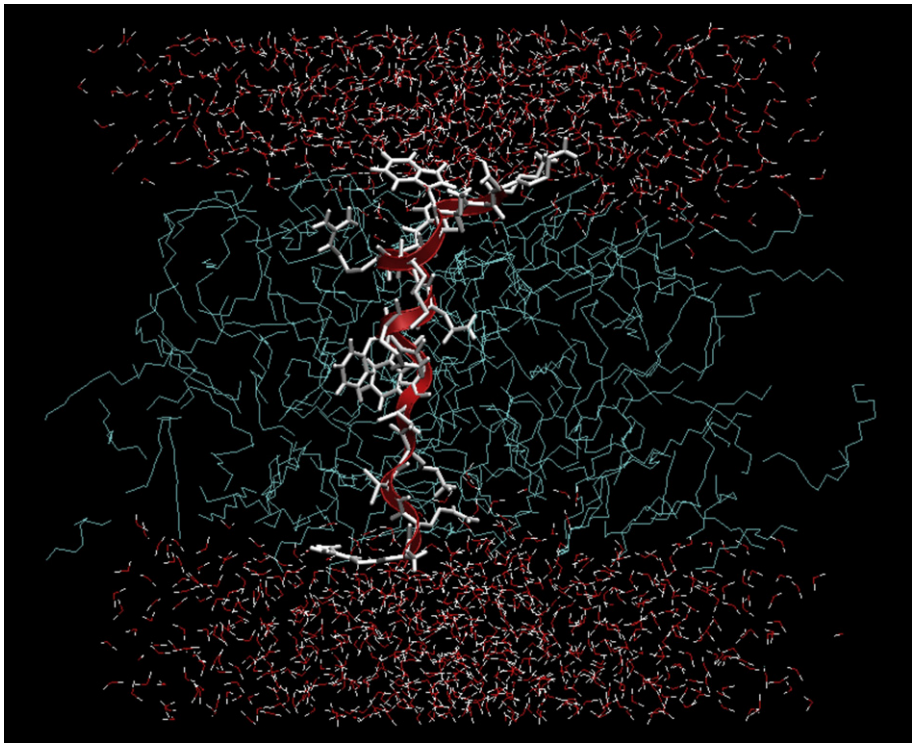

Fig. 2. Snapshot of the location of peptide 6 taken at the end of the simulation.

The wheel representation obtained for peptide **4** was very similar to those of **2** and **3** with the only difference that in the case of peptide **4** all the hydrophobic residues were W, being the general distribution of cationic and hydrophobic residues the same. It is interesting to note that the wheel representations obtained for peptides **2**–**4** were closely related to that previously reported for penetratin [13]. Although the antifungal activity against *C. albicans* obtained for peptides **2**–**4** was similar to that previously reported for penetratin, the antifungal effect obtained against *C. neoformans* for peptide **4** was slightly lower with respect to peptides **1**–**3**. In contrast, the wheel representation obtained for peptide **5** displayed a clearly more extended 'charged face', making the general distribution of this peptide more 'cationic' in relation to peptides **2**–**4**. This is in agreement with Tat which comprises eight cationic out of its twelve amino acid residues, whereas penetratin and peptides **2**–**4** possess only seven cationic out of the sixteen amino acids in total.

It is clear that not only the conformational aspects but the electronic properties of these peptides are determinant for the antifungal activities. Thus, knowledge of the stereoelectronic attributes and properties of these analogues of penetratin and Tat will contribute significantly to the elucidation of the structural requirements to produce the antifungal activity. MEP maps are of particular value because they allow the visualization and assessment of the capacity of a molecule to interact electrostatically with a putative-binding site [32]. MEP can be interpreted in terms of a stereoelectronic pharmacophore condensing all available information on the electrostatic forces underlying affinity and specificity. More positive potentials reflect nucleus predominance while less positive values represent rearrangements of electronic charges and lone pairs of electrons. The fundamental application of this study is the analysis of non-covalent interactions [32b], mainly by investigating the electronic distribution in the molecule. Thus, this methodology was used to evaluate the electronic distribution around molecular surface for the peptides reported here. To better appreciate the electronic behaviour of peptide **2**, and by considering that two different faces were signalled (Fig. 4), we present the MEP of this peptide showing both faces. Fig. 5 (top moiety) shows the 'charged face', characterized by the presence of the four R residues (R1, R4, R11 and R15). Although it is possible to visualize residue R16 near this face, this residue is somewhat shifted in direction to the uncharged face. It has been previously reported that peptide–lipid association occurs through the formation of salt bridges between the positively charged residues K4, R11 and K15 and the lipid phosphate groups [43]. In addition, previous studies on tryptophan fluorescence have

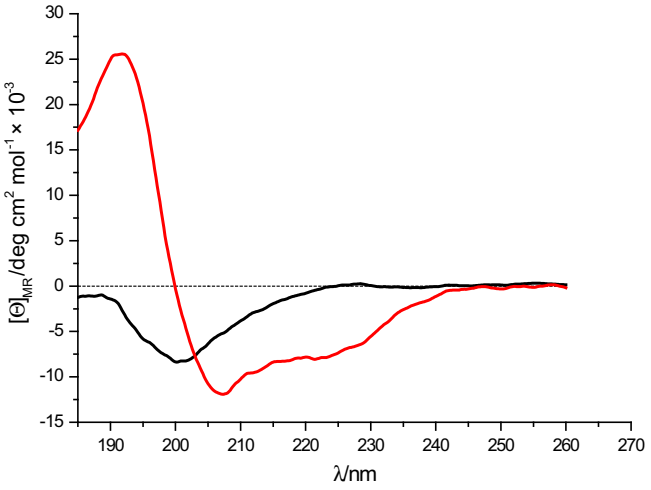

Fig. 3. The CD spectrum of peptide 6 (HFRWRQIKIWFQNRRM[O]KWKK-NH_2) in water (black line) and in TFE/H2O (3:7) (red curve) (For interpretation of the references to colour in this figure legend, the reader is referred to the web version of this article).

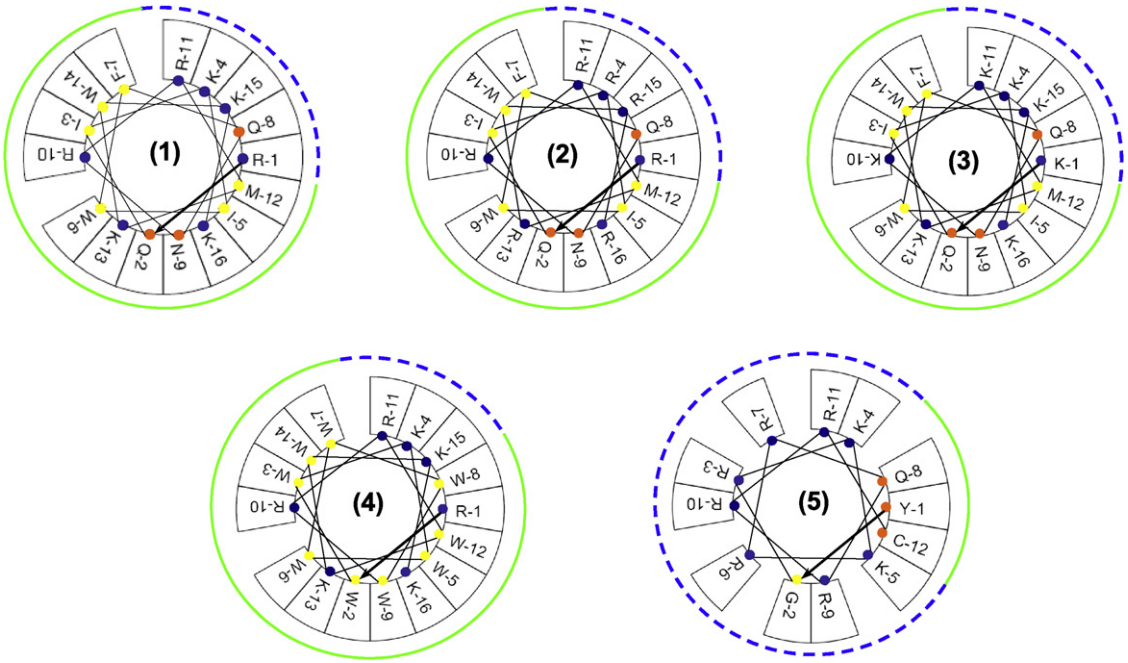

Fig. 4. Edmundson wheel representations of peptides 1–5. The number in the center of the wheel corresponds to the peptide number. The "charged" and "non-charged" faces are shown in blue dash lines and full green lines, respectively. Positively charged amino acids are denoted with blue dots, the polar with orange and the hydrophobic with yellow (For interpretation of the references to colour in this figure legend, the reader is referred to the web version of this article.).

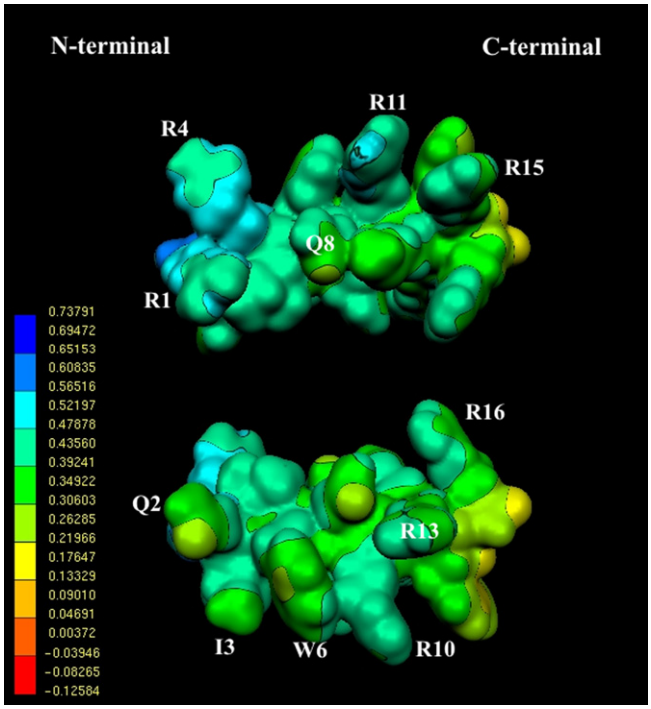

Fig. 5. Electrostatic potential-encoded electron density surfaces of peptide 2: 'charged face' (top moiety) and 'non-charged face' (bottom moiety). The surfaces were generated with GAUSSIAN 03 using RHF/6-31G single point calculations. The coloring electrostatic potential in red is indicating the strongest attraction to a positive point charge whereas blue is indicating the strongest repulsion. The electrostatic potential is the energy of interaction of the positive point charge with the nuclei and electrons of a molecule. It provides a representative measure of overall molecular charge distribution. The colour-code is shown at the left (For interpretation of the references to colour in this figure legend, the reader is referred to the web version of this article.).

shown the importance of peptide positively charged residues for the initial binding to negatively charged vesicles since double R/K→A mutations, involving residues K4/R10/R11/K13/K15 significantly decreased the binding affinity [44]. The MEP of **2** suggests that the above mentioned residues (R1, R4, R11 and R15) might be responsible for the initial binding. Although the main positive potentials (V(r) ranging from 0.73 to 0.47 el.au^{-3}) are concentrated on this side, it should be noted that there is a relatively homogeneous distribution of positively charged residues along the entire helical structure. Thus, residues R16, R13 and R10 are strategically located in an alternated manner within the uncharged face. Fig. 5 (bottom moiety) displays the 'uncharged face'. It appears that a kind of cation-π interaction through W6/R10 takes place in this portion of **2**. The cation-π interaction between residues at the i and $(i+4)$ positions is recognized as an important non-covalent binding interaction which may commonly occur within α-helices [45]. Lensink et al. [43] reported that hydrophobic residues could protect the peptide from the water phase. A clear hydrophobic interaction between I3 and W6 might also be appreciated in Fig. 5 (bottom moiety). It appears that charge neutralization is required for a deeper insertion of these peptides into the hydrophobic core of the membrane. The extended uncharged face alternating cationic residues among the hydrophobic one observed in the MEP of these peptides appears to be operative in this sense.

Fig. S1 and S2 (in Supplementary data) show the MEP obtained for peptides **3** and **4**, respectively. The MEP of penetratin (**1**) was also included in this analysis for comparative purposes (Fig. S3 in Supplementary data). This MEP was previously reported in reference 13; however, in this work this MEP was recalculated and plotted using the same scale used for the rest of peptides reported here. Comparing the MEP obtained for peptides **1**–**4,** it is clear that all of them possess a closely related electronic distribution which might explain, at least in part, the similar antifungal activity obtained for these peptides.

Fig. 6 shows the MEP obtained for peptide **5**. This surface displays a more extended positively charged face with respect to

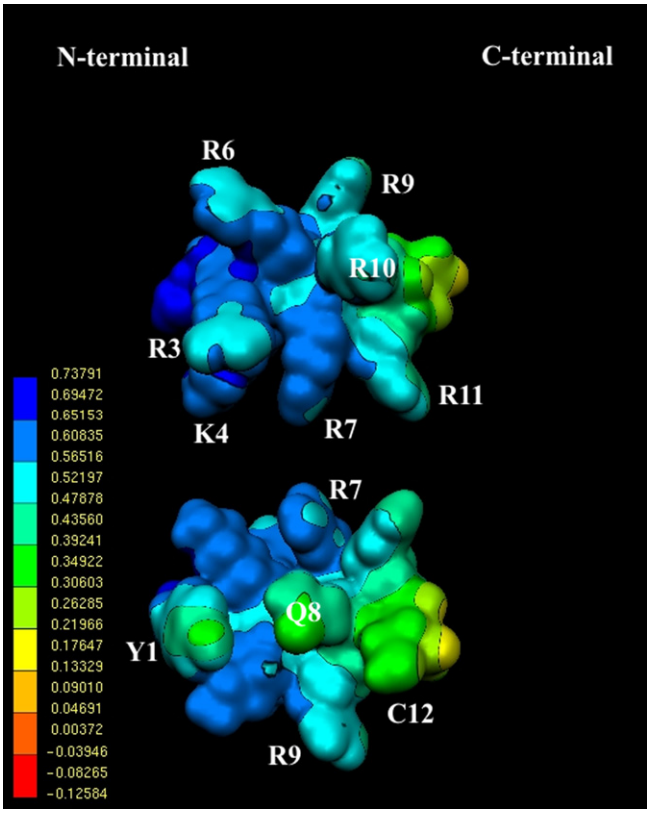

Fig. 6. Electrostatic potential-encoded electron density surfaces of peptide 5: 'charged face' (top moiety) and 'non-charged face' (bottom moiety).

the other peptides. Eight cationic residues, namely R3, K4, K5, R6, R7, R9, R10 and R11 are located in this section. All of them, except K5 might be observed in Fig. 6 (top moiety). A very extensive deep blue zone with potential values in the order of 0.70 el au^{-3} clearly dominates this surface. Fig. 6 shows that peptide **5** is 'too cationic' with respect to penetratin and peptides **2**–**4**. Previously reported MD simulations indicated that the aromatic residues did not contribute to the initial binding, but rather to the subsequent insertion of penetratin between the bilayer head groups, when they shielded the peptide from the aqueous phase [43]. The importance of hydrophobic residues seems to be crucial for the antifungal activity as well. Thus, the different electronic distribution displayed for peptide **5** with respect to the other peptides might be responsible for its lower antifungal activity. These results are in agreement with those previously reported for other so-called 'too cationic' peptides, displaying only marginal antifungal activity [13]. These results are an additional support for the key role of the hydrophobic residues in these peptides acting as antifungal compounds.

In terms of bioavailability, stability and pharmacokinetics, most peptides are as bad as proteins, and, in general, they do not make good drugs unless modified in some way. It is clear that peptides possess significant limitations to be used directly as drugs; however, many of these peptides are excellent starting structures to develop potential new drugs. Therefore, our results must be considered as preliminary results in the lengthy way of designing antifungal leads. Nevertheless, they allowed the identification of a promising 3D pharmacophore for these compounds. In relation to the possible mechanism of action of the peptides reported here, in general cationic peptides possess a relatively non-specific mechanism of action, either causing a detergent-like disruption of the bacterial or fungal cell membrane or forming transient transmembrane pores [46]. However, we have not obtained definitive results about the possible molecular mechanism for these peptides yet.

4. Conclusions

In the present paper, we report the synthesis and antifungal effects of penetratin analogues and Tat peptide. In addition, a conformational and electronic study of these peptides was carried out. Our conformational study from experimental (CD spectroscopy) and theoretical methods (MD calculations using a combined decane/water system simulating the biological environment) indicated that these peptides adopt a helical secondary structure as the preferred form in an environment of low polarity.

The analogues of penetratin reported here (compounds **2**–**4** and **6**) displayed antifungal effect against *C. albicans* and *C. neoformans* being peptide **6** (HFRWRQIKIWFQNRRM[O]KWKK-NH_2) the most active peptide in this series. In contrast, Tat (peptide **5**), a well-known cell penetrating peptide, do not show a significant antifungal activity against fungus tested here. It appears that the lack of hydrophobic residues in this peptide might be responsible for its lower bioactivity.

The antifungal activity obtained for these peptides is very interesting *per se*, but considering their cell penetrating properties, they are also excellent candidates to be used as carriers of other antifungal compounds, thus enhancing their pharmacokinetic aspects.

In addition, the results reported here provide an additional support for the pharmacophoric patron previously reported for penetratin and its derivatives. This pattern suggests a particular combination of cationic and hydrophobic residues, adopting a definite spatial ordering which appears to be the key factor for the transition from the hydrophilic to the hydrophobic phase. This transition appears to be a necessary step to produce the antifungal activity. We believe that our results might contribute to the understanding of the minimal structural requirements for the antifungal effects of peptides reported here.

Acknowledgements

This work is part of the Hungarian–Argentine Intergovernmental S&T Cooperation Programme. This research was partially supported by grants from Universidad Nacional de San Luis and it is part of the Iberoamerican Project X.7 PIBEAFUN (Search and development of new antifungal part of the Iberoamerican Program of Science and Technology for the Development (CYTED)). R.D.E. is a member of the CONICET (Argentina) staff.

Appendix. Supplementary material

Supplementary data related to this article can be found online at doi:10.1016/j.ejmech.2010.10.025.

References

[1] a) M.A. Pfaller, D.J. Diekema, Epidemiology of invasive candidiasis: a persistent public health problem, J. Clin. Microbiol. Rev. 20 (2007) 133–163;
b) M.A. Pfaller, D.J. Diekema, Rare and emerging opportunistic fungal pathogens: Concern for resistance beyond *Candida albicans* and *Aspergillus fumigatus*, J. Clin. Microbiol. 42 (2004) 4419–4431.
[2] T.J. Walsh, A. Groll, J. Hiemenz, R. Fleming, E. Roilides, E. Anaissie, Infections due to emerging and uncommon medically important fungal pathogens, Clin. Microbiol. Infect. 10 (2004) 48–66.
[3] a) D.J. Sheehan, C.A. Hitchcock, C.M. Sibley, Current and emerging azole antifungal agents, Clin. Microbiol. Rev. 12 (1999) 40–79;
b) B.J. Kullberg, B.E. De Pauw, Therapy of invasive fungal infections, Neth. J. Med. 55 (1999) 118–127.
[4] B.D. Alexander, J.R. Perfect, Antifungal resistance trends towards the year 2000. Implications for therapy and new approaches, Drugs 54 (1997) 657–678.

[5] P.K. Mukherjee, J. Chandra, D.M. Kuhn, M.A. Ghannoum, Mechanism of fluconazole resistance in *Candida albicans* biofilms: phase-specific role of efflux pumps and membrane sterols, Infect. Immun. 71 (2003) 4333–4340.
[6] D.P. Kontoyiannis, E. Mantadakis, G. Samonis, Systemic mycoses in the immunocompromised host: an update in antifungal therapy, J. Hosp. Infect. 53 (2003) 243–258.
[7] A. Polak, The past, present and future of antimycotic combination therapy, Mycoses 42 (1999) 355–370.
[8] J. Bartroli, E. Turmo, M. Algueró, E. Boncompte, M.L. Vericat, L. Conte, J. Ramis, M. Merlos, J. García-Rafanell, J. Forn, New azole antifungals. 3. Synthesis and antifungal activity of 3- substituted-4(3H)-quinazolinones, J. Med. Chem. 41 (1998) 1869–1882.
[9] R.E.W. Hancock, Peptide antibiotics, Lancet 349 (1997) 418–422.
[10] R.E.W. Hancock, A. Patrzykat, Clinical development of cationic antimicrobial peptides: from natural to novel antibiotics, Curr. Drug Targets Infect. Disord. 2 (2002) 79–83.
[11] D. Derossi, A.H. Joliot, G. Chassaing, A. Prochiantz, The third helix of the Antennapedia homeodomain translocates through biological membranes, J. Biol. Chem. 269 (1994) 10444–10450.
[12] D. Derossi, S. Calvet, A. Trembleau, A. Brunissen, G. Chassaing, A. Prochiantz, Cell internalization of the third helix of the antennapedia homeodomain is receptor-independent, J. Biol. Chem. 271 (1996) 18188–18193.
[13] M.F. Masman, A.M. Rodríguez, M. Raimondi, S.A. Zacchino, P.M.G. Luiten, C. Somlai, T. Kortvelyesi, B. Penke, R.D. Enriz, Penetratin and derivatives acting as antifungal agents, Eur. J. Med. Chem. 44 (2009) 212–228.
[14] F.M. Garibotto, A.D. Garro, M.F. Masman, A.M. Rodríguez, P.G.M. Luiten, M. Raimondi, S.A. Zacchino, C. Somlai, B. Penke, R.D. Enriz, New small-size peptides possessing antifungal activity, Bioorg. Med. Chem. 18 (2010) 158–167.
[15] E. Kaiser, R.L. Colescott, C.D. Bossiuger, P.I. Cook, Color test for detection of free terminal amino groups in the solid-phase synthesis of peptides, Anal. Biochem. 34 (1970) 595–598.
[16] Clinical and Laboratory Standards Institute (CLSI, formerly National Committee for Clinical and Laboratory Standards NCCLS), in: Wayne (Ed.), second ed., Method M27-A2, vol. 22, 2002, pp. 1–29.
[17] A. Liwo, A. Tempczyk, S. Oldziej, M.D. Shenderovich, V.J. Hruby, S. Talluri, J. Ciarkowski, S. Kasprzykowski, L. Lankiewicz, Z. Grzonka, Exploration of the conformational space of oxytocin and arginine-vasopressin using the electrostatically driven monte carlo and molecular dynamics methods, Biopolymers 38 (1996) 157–175.
[18] a) D.R. Ripoll, H.A. Scheraga, On the multiple-minima problem in the conformational analysis of polypeptides. II. An electrostatically driven Monte Carlo method–tests on poly(l-alanine), Biopolymers 27 (1988) 1283–1303;
b) D.R. Ripoll, H.A. Scheraga, On the multiple-minima problem in the conformational analysis of polypeptides. IV. Application of the electrostatically driven Monte Carlo method to the 20-residue membrane-bound portion of melittin, Biopolymers 30 (1990) 165–176.
[19] H.A. Scheraga, D.R. Ripoll, A. Liwo, C. Czaplewski, User Guide ECEPPAK and ANALYZE Programs.
[20] G. Némethy, K.D. Gibson, K.A. Palmer, C.N. Yoon, G. Paterlini, A. Zagari, S. Rumsey, H.A. Scheraga, Energy parameters in polypeptides. 10. Improved geometrical parameters and nonbonded interactions for use in the ECEPP/3 algorithm, with application to proline-containing peptides, J. Phys. Chem. 96 (1992) 6472–6484.
[21] a) J. Vila, R.L. Williams, M. Vásquez, H.A. Scheraga, Empirical solvation models can be used to differentiate native from near-native conformations of bovine pancreatic trypsin inhibitor, Proteins: Struct. Funct. Genet. 10 (1991) 199–218;
b) R.L. Williams, J. Vila, G. Perrot, H.A. Scheraga, Empirical solvation models in the context of conformational energy searches: application to bovine pancreatic trypsin inhibitor, Proteins: Struct. Funct. Genet. 14 (1992) 110–119.
[22] J.A. Bombasaro, M.F. Masman, L.N. Santagata, M.L. Freile, A.M. Rodríguez, R.D. Enriz, A comprehensive conformational analysis of bullacin B, a potent inhibitor of complex I. Molecular dynamics simulations and *ab initio* calculations, J. Phys. Chem. A 112 (2008) 7426–7438.
[23] H.J.C. Berendsen, D. van der Spoel, R. van Drunen, GROMACS: a message-passing parallel molecular dynamics implementation, Comput. Phys. Commun. 91 (1995) 43–56.
[24] W.L. Jorgensen, J. Chandrasekhar, J.D. Madura, R.W. Impey, M.L. Klein, Comparison of simple potential functions for simulating liquid water, J. Chem. Phys. 79 (1983) 926–935.
[25] A.R. Van Buuren, H.J.C. Berendsen, Molecular dynamics simulation of the stability of a 22-residue [fx1]-helix in water and 30% trifluoroethanol, Biopolymers 33 (1993) 1159–1166.
[26] T. Darden, D. York, L. Pedersen, Particle mesh Ewald: an $N\cdot\log(N)$ method for Ewald sums in large systems, J. Chem. Phys. 98 (1993) 10089–10092.
[27] K. Zimmerman, ORAL: all purpose molecular mechanics simulator and energy minimizer, J. Comput. Chem. 12 (1991) 310–319.
[28] H.J.C. Berendsen, J.P.M. Postma, W.F. van Gunsteren, A. DiNola, J.R. Haak, Molecular dynamics with coupling to an external bath, J. Chem. Phys. 81 (1984) 3684–3690.
[29] S. Miyamoto, P.A. Kollman, Settle: an analytical version of the SHAKE and RATTLE algorithm for rigid water models, J. Comput. Chem. 13 (1992) 952–962.
[30] B. Hess, H. Bekker, H.J.C. Berendsen, J.G.E.M. Fraaije, LINCS: a linear constraint solver for molecular simulations, J. Comput. Chem. 18 (1997) 1463–1472.
[31] M.J. Frisch, G.W. Trucks, H.B. Schlegel, G.E. Scuseria, M.A. Robb, J.R. Cheeseman, J.A. Montgomery Jr., T. Vreven, K.N. Kudin, J.C. Burant, J.M. Millam, S.S. Iyengar, J. Tomasi, V. Barone, B. Mennucci, M. Cossi, G. Scalmani, N. Rega, G.A. Petersson, H. Nakatsuji, M. Hada, M. Ehara, K. Toyota, R. Fukuda, J. Hasegawa, M. Ishida, T. Nakajima, Y. Honda, O. Kitao, H. Nakai, M. Klene, X. Li, J.E. Knox, H.P. Hratchian, J.B. Cross, C. Adamo, J. Jaramillo, R. Gomperts, R.E. Stratmann, O. Yazyev, A.J. Austin, R. Cammi, C. Pomelli, J.W. Ochterski, P.Y. Ayala, K. Morokuma, G.A. Voth, P. Salvador, J.J. Dannenberg, V.G. Zakrzewski, S. Dapprich, A.D. Daniels, M.C. Strain, O. Farkas, D.K. Malick, A.D. Rabuck, K. Raghavachari, J.B. Foresman, J.V. Ortiz, Q. Cui, A.G. Baboul, S. Clifford, J. Cioslowski, B.B. Stefanov, G. Liu, A. Liashenko, P. Piskorz, I. Komaromi, R.L. Martin, D.J. Fox, T. Keith, M.A. Al-Laham, C.Y. Peng, A. Nanayakkara, M. Challacombe, P.M.W. Gill, B. Johnson, W. Chen, M.W. Wong, C. Gonzalez, J.A. Pople, Gaussian 03, Revision B.05. Gaussian, Inc., Pittsburgh PA, 2003.
[32] a) P. Politzer, D.G. Truhlar, Chemical Applications of Atomic and Molecular Electrostatic Potentials. Plenum Press, New York, 1993;
b) G. Náray-Szabó, G.G. Ferenczy, Molecular electrostatics, Chem. Rev. 95 (1995) 829–847.
[33] P. Flükiger, H.P. Lüthi, S. Portmann, J. Weber, MOLEKEL 4.0. Swiss Center for Scientific Computing, Manno, Switzerland, 2000.
[34] a) T. Letoha, S. Gaá, C. Somlai, A. Czajlik, A. Perczel, B. Penke, Membrane translocation of penetratin and its derivatives in different cell lines, J. Mol. Recognition 16 (2003) 272–279;
b) A. Czajlik, E. Meskó, B. Penke, A. Perczel, Investigation of penetratin peptides. Part 1. The environment dependent conformational properties of penetratin and two of its derivatives, J. Pept. Sci. 8 (2002) 151–171.
[35] P.M. Fischer, N.Z. Zhelev, S. Wang, J.E. Melville, R. Fahraeus, D.P. Lane, Structure–activity relationship of truncated and substituted analogues of the intracellular delivery vector penetratin, J. Pept. Res. 55 (2000) 163–172.
[36] E. Vivès, P. Brodin, B. Lebleu, A truncated HIV-1 Tat protein basic domain rapidly translocates through the plasma membrane and accumulates in the cell nucleus, J. Biol. Chem. 272 (1997) 16010–16017.
[37] M.F. Masman, A.M. Rodríguez, L. Svetaz, S.A. Zacchino, C. Somlai, I.G. Csizmadia, B. Penke, R.D. Enriz, Synthesis and conformational analysis of His-Phe-Arg-Trp-NH_2 and analogues with antifungal properties, Bioorg. Med. Chem. 14 (2006) 7604–7614.
[38] M. Olivella, A.M. Rodríguez, S.A. Zacchino, C. Somlai, B. Penke, V. Farkas, A. Perczel, R.D. Enriz, New antifungal peptides. Synthesis, bioassays and initial structure prediction by CD spectroscopy, Bioorg. Med. Chem. Lett. 20 (2010) 4808–4811.
[39] J.M. Peloponese, C. Gregoire, S. Opi, D. Esquieu, J. Sturgis, É Lebrun, É Meurs, Y. Collette, D. Olive, A.M. Aubertin, M. Witvrow, C. Pannecouque, E. De Clercq, C. Bailly, J. Lebreton, E.P. Loret, $^{1}H-^{13}C$ nuclear magnetic resonance assignment and structural characterization of HIV-1 Tat protein, C.R. Acad. Sci. 323 (2000) 883–894.
[40] Z. Salamon, G. Lindblom, G. Tollin, Plasmonwaveguide resonance and impedance spectroscopy studies of the interaction between penetratin and supported bilayer membranes, Biophys. J. 84 (2003) 1796–1807.
[41] S. Yesylevskyy, S.J. Marrink, A.E. Mark, Alternative mechanisms for the interaction of the cell-penetrating peptides penetratin and the Tat peptide with lipid bilayers, Biophys. J. 97 (2009) 40–49.
[42] E. Bellet-Amalric, D. Blaudez, B. Desbat, F. Graner, F. Gauthier, A. Renault, Interaction of the third helix of Antennapedia homeodomain and a phospholipid monolayer, studied by ellipsometry and PM-IRRAS at the air-water interface, Biochim. Biophys. Acta Biomembranes 1467 (2000) 131–143.
[43] M.F. Lensink, B. Christiaens, J. Vandekerckhove, A. Prochiantz, M. Rosseneu, Penetratin-membrane association: W48/R52/W56 shield the peptide from the aqueous phase, Biophys. J. 88 (2005) 939–952.
[44] B. Christiaens, J. Grooten, M. Reusens, A. Joliot, M. Goethals, J. Vandekerckhove, A. Prochiantz, M. Rosseneu, Membrane interaction and cellular internalization of penetratin peptides, Eur. J. Biochem. 271 (2004) 1187–1197.
[45] J.P. Gallivan, D.A. Dougherty, Cation-π interactions in structural biology, Proc. Natl. Acad. Sci. USA 96 (1999) 9459–9464.
[46] a) Y. Shai, Mode of action of membrane active antimicrobial peptides, Biopolymers 66 (2002) 236–248;
b) H.W. Huang, Action of antimicrobial peptides: two-state model, Biochemistry 39 (2000) 8347–8352.